JOURNAL OF VIROLOGY, June 1996, p. 3876–3886 Vol. 70, No. 6
0022-538X/96/$04.00+0

Coxsackie B3 Virus Protein 2B Contains a Cationic Amphipathic Helix That Is Required for Viral RNA Replication

FRANK J. M. VAN KUPPEVELD,* JOCHEM M. D. GALAMA, JAN ZOLL, PATRICK J. J. C. VAN DEN HURK, AND WILLEM J. G. MELCHERS

Department of Medical Microbiology, University of Nijmegen, 6500 HB Nijmegen, The Netherlands

Received 18 September 1995/Accepted 12 March 1996

Enterovirus protein 2B has been shown to increase plasma membrane permeability. We have identified a conserved putative amphipathic α-helix with a narrow hydrophilic face and an arrangement of cationic residues that is typical for the so-called lytic polypeptides. To examine the functional and structural roles of this putative amphipathic α-helix, we have constructed nine coxsackie B3 virus mutants by site-directed mutagenesis of an infectious cDNA clone. Six mutants contained substitutions of the charged residues in the hydrophilic face of the α-helix. Three mutants contained insertions of leucine residues between the charged residues, causing a disturbance of the amphipathic character of the α-helix. The effect of the mutations on virus viability was assayed by transfection of cells with copy RNA transcripts. The effect on positive-strand RNA replication was examined by introduction of the mutations in a subgenomic luciferase replicon and analysis of luciferase accumulation following the transfection of BGM cells with RNA transcripts. It is shown that both the amphipathy of the domain and the presence of cationic residues in the hydrophilic face of the α-helix are required for virus growth. Mutations that disturbed either one of these features caused defects in viral RNA synthesis. In vitro translation reactions and the analysis of viral protein synthesis in vivo demonstrated that the mutations did not affect synthesis and processing of the viral polyprotein. These results suggest that a cationic amphipathic α-helix is a major determinant for a function of protein 2B, and possibly its precursor 2BC, in viral RNA synthesis. The potential role of the amphipathic α-helix in the permeabilization of cellular membranes is discussed.

Enteroviruses contain a single-stranded RNA genome of positive polarity with a genetically encoded poly(A) tail at their 3′ end. The viral RNA (vRNA) directs the synthesis of a single polyprotein which is processed by the virally encoded proteases $2A^{pro}$, $3C^{pro}$, and $3CD^{pro}$. The P1 region of the genome encodes the structural capsid proteins. The proteins encoded by the P2 and P3 regions have been implicated in viral replication (reviewed in reference 47). Replication starts by the formation of a complementary negative-stranded RNA molecule which serves as the template for the synthesis of progeny viral positive-stranded RNAs (5). The proteins encoded by the P3 region are physically involved in the process of positive-strand RNA synthesis (3, 22, 42, 43), which occurs in replication complexes on virus-induced cytoplasmic membrane vesicles (8). The proteins encoded by the P2 region are involved in the induction of some of the structural and metabolic alterations that occur in the infected cell. Protein $2A^{pro}$ induces the cleavage of the 220-kDa component of the eucaryotic initiation factor eIF-4F, which results in an inhibition of cap-dependent host cell translation (18, 20, 29). Translation of viral RNA is not affected, because it is initiated via a cap-independent binding of ribosomes to secondary structures in the 5′ nontranslated region (26, 35). Precursor protein 2BC has been implicated in the rearrangement of membranes and the generation of the membrane vesicles at which positive-strand RNA synthesis occurs (7–10). The observation that protein 2C alone is also capable of inducing this rearrangement (2, 14) is hampered by the use of a recombinant vaccinia virus, which modifies vesicular traffic itself. Protein 2C is a nucleoside triphosphatase (33, 39) with RNA binding capacities (39) that is localized at the outer surface of the virus-induced membrane vesicles (7, 9, 10), which suggests that protein 2C may be involved in the structural organization of the viral replication complex by attaching the vRNA to the vesicular membranes.

Two other metabolic alterations that occur during an enterovirus infection are the inhibition of cellular protein secretion (16) and the permeabilization of the plasma membrane (12). Upon expression of individual poliovirus proteins, Doedens and Kirkegaard found that protein 2B, as well as its precursor 2BC, was capable of inducing both alterations (16). The significance of these alterations, which become evident from the third-hour postinfection, for virus replication is unclear. The block in protein secretion may be involved in the accumulation of cytoplasmic vesicles for vRNA synthesis. Apart from this, the inhibition of cellular protein secretion may interfere with host cell responses such as interferon secretion and antigen presentation. Modification of membrane permeability occurs in the late phase of infection of most cytolytic viruses and requires viral gene expression (reviewed by Carrasco et al. in reference 13). The modification is such that gradients of monovalent cations are gradually destroyed and compounds that normally do not pass the membrane leak out of the cell or leak into the cytoplasm. Carrasco et al. (13) have suggested that the resulting influx of sodium ions may be involved in the virus-induced shutoff of host cell translation, because the cleavage of the 220-kDa component of eIF-4F may not be sufficient to completely shut off host cell translation (11, 36). High concentrations of sodium are inhibitory to host mRNA translation, whereas viral RNA is optimally translated under these altered conditions by the use of specialized structures in the 5′ nontranslated region (13). Another function of the membrane modification may be the induction of the cell lysis needed to liberate newly formed virus particles.

* Corresponding author. Mailing address: Department of Medical Microbiology, University of Nijmegen, P.O. Box 9101, 6500 HB Nijmegen, The Netherlands. Phone: 31 24 3614356. Fax: 31 24 3540216. Electronic mail address: KUNAZAG3@CAOS.KUN.NL.

Enterovirus protein 2B and its precursor 2BC are localized exclusively at the outer surface of the virus-induced membrane vesicles at which positive-strand synthesis occurs (7, 8). Genetic evidence suggests that protein 2B, or possibly its precursor 2BC, is required for a *cis*-acting function in vRNA replication (27, 46). The expression of protein 2B in both bacteria and eucaryotic cells led to an increase in cell membrane permeability, which suggests that protein 2B possesses membrane-active or ionophoric properties. Both functions require amphipathic helix motifs with high helical hydrophobic moments (19). We have identified a well-conserved amphipathic helix motif in enterovirus protein 2B with a narrow hydrophilic face and an arrangement of cationic residues that is typical for the so-called lytic polypeptides. The conserved nature of this structural domain is indicative of an important role in the functioning of protein 2B. To examine the structural and functional roles of this putative amphipathic α-helix, we have constructed mutant coxsackie B3 virus cDNAs that contained substitutions of the charged residues in the hydrophilic face or insertions of hydrophobic leucine residues that disturb the amphipathic character of the helix. The effects of the mutations on virus viability, RNA synthesis, viral protein synthesis, and polyprotein processing were examined. Our results indicate that a cationic amphipathic α-helix is indeed required for a function of protein 2B, and possibly also its precursor 2BC, in vRNA synthesis but not for viral protein synthesis or polyprotein processing. The potential role of the amphipathic α-helix in the permeabilization of the plasma membrane is discussed.

MATERIALS AND METHODS

Cells and viruses. Virus propagations, endpoint titrations, and RNA transfections were performed with Buffalo green monkey (BGM) cells. Plaque assays were performed with Vero cells. The cells were grown in minimal essential medium (MEM) supplemented with 10% fetal bovine serum. After infection, the cells were fed with MEM supplemented with 3% fetal bovine serum. After transfection, the cells were fed with MEM containing 10% fetal bovine serum.

Oligonucleotide-directed site-specific mutagenesis. In vitro mutagenesis was performed with a subgenomic pALTER phagemid clone containing nucleotides (nt) 2080 to 4947 of coxsackie B3 virus (CBV3) (46), using the Altered Sites in vitro mutagenesis system (Promega) according to the instructions of the manufacturer. The nucleotide sequences of the antisense synthetic oligonucleotides (Isogen Bioscience, The Netherlands) used for construction of the mutants (shown in parentheses) are as follows: 5′-TGATATTATCCTAACTAAGG CTCTTAGAGATCTCTCTAAGAT-3′ (2B-K[41,44,48]R [This mutant contains K-to-R mutations at positions 41, 44, and 48]); 5′-TGATATTATCTCAACTAAG GCCTCTAGAGATTCCTCTAAGAT-3′ (2B-K[41,44,48]E); 5′TAAGGCTTTTA GAGAGAGCTCTAAGATGGAGTC-3′ (2B-K[41]L); 5′-TATCTTAACTAAG GCTAGCAGAGAGAGCTCTAAGATGGAGTC-3′ (2B-K[41,44]L); 5′-TTTTA GAGATTTCTTTAAAATGGAGTCTTGACC-3′ (2B-E[40]K); 5′-GGCTTTTAG AGATTTGTCTAGAATGGAGTCTTGACCCAC-3′ (2B-E[40]D); 5′-AACTAA GGCTTTTAGAGACTTAAGCTCTAAGATGGAGTCTTGACC-3′ (2B-ins[41] L); 5′-TATTATCTTAACTAAGGCCTTAAGTAGAGATTTCTCTAAGATGG A-3′ (2B-ins[44]L); and 5′-TACTAAGGCTGATATTATCTTAAGAACTAAG GCTTTTAGAGATTT-3′ (2B-ins[48]L). Each of these oligonucleotides created a novel restriction endonuclease site. Mutant clones were identified by restriction enzyme analysis. The nucleotide sequences of the mutant pALTER clones were verified by dideoxy chain termination sequencing of plasmid DNA with the oligonucleotide 5′-CCATTCAATGAATTTCTG-3′ (nt 4117 to 4134), using the Ampli Cycle sequencing kit according to the instructions of the manufacturer (Perkin-Elmer). The 402-bp *Spe*I-to-*Bss*HII fragments of the mutant clones were introduced in the unique *Spe*I (nt 3837) and *Bss*HII (nt 4238) sites of plasmid pCB3/T7 which contains a cDNA of CBV3 (strain Nancy) behind a T7 RNA polymerase promoter (28).

Construction of plasmid 2B-bomII. Nucleotides 3862 to 3906 of pCB3/T7 (coding sequence for protein 2B amino acids [aa] 40 to 55) were replaced by 45 nt encoding 15 aa of bombolitin II by using PCR with the synthetic 105-mer 5′-GAATCACTAGTGGGTCAAGACTCCATCTTAAGCAAGAT CACCGATATCCTCGCGAAGCTTGGAAAAGTACTGGCCATTGTGGT GAGGAACCACGATGACCTGATC-3′ (nt 3832 to 3936; nucleotides encoding the bombolitin II amino acids are underlined) and the oligonucleotide 5′-TTGGGATGGCGCGCTCTGCTC-3′ (complementary to nt 4231 to 4251). PCRs were performed with ULTma DNA polymerase (Perkin-Elmer), a thermostable DNA polymerase with proofreading activity, and pCB3/T7 DNA as the template DNA. The thermal profile consisted of 20 cycles of denaturation at 94°C for 1 min, primer annealing at 55°C for 1 min, and primer extension at 72°C for 2 min. The resulting PCR product was cut with *Spe*I and *Bss*HII and cloned in pCB3/T7 cut with the same enzymes. The entire introduced fragment was verified by sequence analysis. The resulting plasmid was designated 2B-bomII.

Transfection of cells with copy RNA transcripts. Plasmids were linearized with *Sal*I and transcribed by phage T7 RNA polymerase as described previously (46). The integrity of the RNA transcripts was checked on a 1% agarose gel. BGM cell monolayers grown in 25-cm^2 flasks to a confluency of 70 to 80% were transfected with 5 μg of RNA transcripts by the DEAE-dextran method as described previously (46). After transfection, the cells were incubated at either 33 or 36°C. When virus growth was observed, the cultures were incubated until cytopathic effect was complete. The cultures were then subjected to three cycles of freezing and thawing, and the viruses were aliquoted in stocks of 1 ml and stored at −80°C.

Sequence analysis of the 2B coding region of mutant viruses. Extraction of RNA, cDNA synthesis, and amplification by PCR were performed as described previously (46), using forward primer 5′-TGGTGTCATTGGCATTGTGAC CATGGGGGG-3′ (nt 3648 to 3677) and reverse primer 5′-TTGGGATGGC GCGCTCTGCTC-3′ (nt 4231 to 4251). The resulting 604-bp PCR products were purified by low-melting-point agarose gel electrophoresis. Sequence analysis was performed as described above.

Plaque assays and single-cycle growth analysis. Plaque assays were performed with 100% confluent Vero cell monolayers grown in 6-well plates as described previously (46). For single-cycle infections, 100% confluent BGM cell monolayers grown in 25-cm^2 flasks (5×10^6 cells) were infected with virus at a multiplicity of infection (MOI) of 1 50% tissue culture infective dose per cell for 30 min at room temperature. The cells were grown at 33, 36, or 39°C for 2, 4, 6, or 8 h. Viruses were released by three cycles of freezing and thawing. Viruses were titrated on BGM cell monolayers in 96-well plates, as previously described (46). 50% tissue culture infective dose values were calculated according to the method of Reed and Muench (38).

Analysis of RNA synthesis. To study the effect of the mutations on RNA synthesis, the *Spe*I-to-*Bss*HII fragments of the mutant plasmids were cloned in the chimeric subgenomic replicon pCB3/T7-LUC (46), which contains the firefly luciferase gene in place of the capsid coding P1 region. BGM cell monolayers in 25-cm^2 flasks grown to a confluency of 70 to 80% were transfected with 0.5 μg of T7 RNA polymerase-generated RNA transcripts derived from *Sal*I-linearized pCB3/T7-LUC constructs. The cells were grown at 36°C, and at the indicated times posttransfection they were washed three times with phosphate-buffered saline (PBS) and lysed in 400 μl of lysis buffer. The luciferase activity was measured in a liquid scintillation counter by using the Luciferase Assay System according to the recommendations of the manufacturer (Promega).

In vitro translation reactions. Copy RNA transcripts were synthesized and translated in T7 TNT rabbit reticulocyte lysate (Promega) supplemented with 20% (vol/vol) HeLa cell initiation factors (kindly provided by J. Flanegan, University of Florida). The translation reaction mixtures (20 μl) contained 0.5 μg of circular plasmid DNA and 20 μCi of Tran^{35}S-label (a mixture of [^{35}S]methionine and [^{35}S]cysteine; specific activity, >1,000 Ci/mmol; ICN). After 3 h of incubation at 30°C, RNA was degraded by treatment with RNase T_1 (500 U) and RNase A (5 μg) for 10 min at 30°C. Labeled translation products were analyzed on a 12.5% polyacrylamide gel containing sodium dodecyl sulfate (SDS) (30). The gels were fixed, fluorographed, and exposed to Kodak XAR film at −80°C.

Analysis of viral protein synthesis in vivo. BGM monolayers (2×10^5 cells) were infected with either wild-type or mutant virus at a MOI of 25. At the indicated times postinfection, the cells were washed with PBS and incubated in methionine- and serum-free MEM (Gibco) containing 10 μCi of Tran^{35}S-label. After 30 min, the medium was removed and the cells were lysed in cold lysis buffer containing 500 mM Tris HCl (pH 8.0), 150 mM NaCl, 0.1 mM phenylmethylsulfanyl fluoride, 1% Nonidet P-40, and 0.05% SDS. Labeled proteins were analyzed by polyacrylamide gel electrophoresis as described above.

RESULTS

Identification and classification of a putative amphipathic helix in enterovirus protein 2B. We have searched for the presence of amphipathic helix motifs in CBV3 protein 2B by calculating the mean hydrophobic moment and hydrophobicity of 11-residue windows according to the method of Eisenberg et al. (19). Figure 1 shows that amino acids 37 to 54 form the segment with the highest amphipathic potential. The high hydrophobic moment and the moderate hydrophobicity of the 11-residue segment with the highest hydrophobic moment (aa 40 to 50; moment, 0.67; hydrophobicity, 0.11) are characteristic of surface-seeking amphipathic helices (19), i.e., helices which insert their hydrophobic part in the lipid membrane and expose their hydrophilic part to the aqueous face. Graphic representation with a helical wheel diagram according to Schiffer

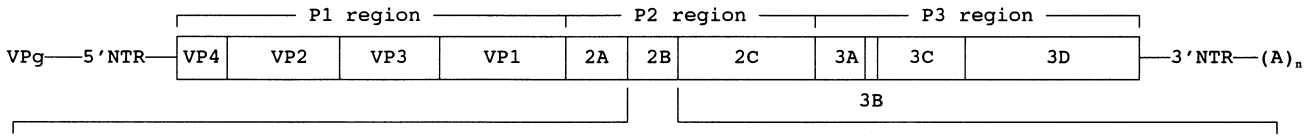

pos	aa	mom.	hyd.	pos	aa	mom.	hyd.	pos	aa	mom.	hyd.
1	G			34	G	0.18	0.06	67	T	0.21 +	0.53
2	V			35	Q	0.13	0.13	68	A	0.11 +	0.74
3	K			36	D	0.15	0.06	69	T	0.05 +	0.68
4	D			37	S	0.15	0.06	70	L	0.13 +	0.59
5	Y			38	I	0.12	0.06	71	A	0.12 +	0.59
6	V	* 0.54	-0.03	39	L	0.34	-0.17	72	L	0.01	0.47
7	E	* 0.56	-0.02	40	E	0.36	-0.15	73	I	0.02	0.46
8	Q	* 0.56	-0.01	41	K	* 0.52	0.02	74	G	0.06	0.41
9	L	* 0.53	0.17	42	S	* 0.50	0.20	75	C	0.13	0.49
10	G	* 0.46	0.24	43	L	** 0.62 +	0.08	76	T	0.32	0.17
11	N	* 0.48	0.26	44	K	** 0.66 +	0.08	77	S	0.34	0.18
12	A	* 0.47	0.27	45	A	** 0.67 +	0.11	78	S	0.34	0.18
13	F	* 0.44	0.33	46	L	** 0.66 +	0.16	79	P	* 0.43	-0.08
14	G	0.41	0.34	47	V	* 0.51 +	0.35	80	W	* 0.52	-0.20
15	S	0.29	0.16	48	K	** 0.61 +	0.46	81	R	0.40	-0.36
16	G	0.34	0.25	49	I	* 0.58 +	0.46	82	W	* 0.47	-0.26
17	F	0.29	0.34	50	I	0.33 +	0.73	83	L	* 0.47	-0.26
18	T	0.39	0.22	51	S	0.35 +	0.77	84	Q	* 0.50	-0.32
19	N	0.33	0.03	52	A	0.35 +	0.77	85	K	* 0.51	-0.31
20	Q	0.37	0.09	53	L	* 0.53 +	0.44	86	Q	* 0.48	-0.36
21	I	0.41	0.03	54	V	* 0.47 +	0.51	87	V	0.23	-0.08
22	C	0.39	0.09	55	I	0.33	0.34	88	S	0.26	-0.03
23	E	0.40	0.07	56	V	0.31	0.14	89	Q	0.17	-0.12
24	Q	0.38	-0.06	57	V	0.37	0.07	90	Y	0.24	0.07
25	V	0.38	-0.05	58	R	0.41	0.11	91	Y	0.15	0.21
26	N	0.37	0.01	59	N	0.41	0.14	92	G	0.07	0.28
27	L	0.33	-0.02	60	H	* 0.48	0.04	93	I	0.26	-0.05
28	L	0.38	0.05	61	D	* 0.52	0.01	94	P	0.23	-0.11
29	K	0.19	0.16	62	D	* 0.43	-0.09	95	M		
30	E	0.18	0.16	63	L	0.40	-0.13	96	A		
31	S	0.22	-0.02	64	I	0.18	0.09	97	E		
32	L	0.17	0.04	65	T	0.26	0.26	98	R		
33	V	0.21	0.06	66	V	0.31	0.35	99	Q		

FIG. 1. Analysis of the hydrophobic moment (amphipathy) and hydrophobicity of CBV3 protein 2B according to the method of Eisenberg et al. (19). The hydrophobic moment (mom.) and hydrophobicity (hyd.) values for each amino acid were calculated by using an 11-residue moving window. A positive hydrophobicity value indicates a hydrophobic nature. Single and double asterisks indicate one and two standard deviations, respectively, above the average amphipathy of the Protein Identification Resource Database (1989). A plus sign indicates that the 11-residue window satisfies the criteria for membrane binding according to the method of Eisenberg et al. (19). At the top of the figure is shown the 7.5-kb single-stranded RNA genome of CBV3, containing (from 5′ to 3′) the 5′ nontranslated region (NTR) with protein VPg covalently bound at its 5′ end; the polyprotein-encoding region (boxed), which can be divided into the structural P1 protein region and the nonstructural P2 and P3 protein regions; and the 3′ NTR containing a polyadenylate tract at its 3′ end.

and Edmundson (40) shows that this segment forms a putative amphipathic α-helix with a narrow hydrophilic face on one side of the helix (Fig. 2A). The distribution of charged residues (three lysines and one glutamic acid) on the hydrophilic face is well conserved among all enteroviruses, except that bovine enterovirus protein 2B contains arginines rather than lysines at positions 44 and 48 (Fig. 2A). The hydrophilic face of poliovirus protein 2B is somewhat larger because of the occurrence of polar asparagine and serine residues at aa 43 and 50, respectively. On the basis of their physical-chemical and structural properties, amphipathic helices are grouped into seven classes (41). The arrangement of the charged residues in the putative amphipathic helix of CBV3 protein 2B is typical for the class of so-called lytic polypeptides. These lytic polypeptides form a group of small cationic amphipathic α-helical peptides that are characterized by narrow polar faces with intermediate charge densities, the occurrence of four times as many positively charged residues as negatively charged residues, and the occurrence of mainly lysine residues in the hydrophilic face (mean lysine/arginine ratio = 30). Figure 2B shows examples of helical wheel diagrams of two lytic polypeptides: bombolitin II (4) and mastoporan (23).

Construction of mutations in the putative amphipathic helix of CBV3 protein 2B. The function and the structural requirements of the putative amphipathic helix in CBV3 protein 2B were examined by a genetic analysis. A total of nine mutants, containing either substitution or insertion mutations, were generated by site-directed mutagenesis. The mutations were verified by sequence analysis and introduced in the infectious cDNA clone pCB3/T7. The genotype of the mutant plasmids and the effects of the mutations on mean hydrophobic moment and hydrophobicity are shown in Fig. 3A. Two mutants were constructed to examine the requirement for lysine residues at aa 41, 44, and 48. In these mutants, the lysine residues were replaced with either arginine residues (2B-K[41,44,48]R) or negatively charged glutamic acid residues (2B-K[41,44,48]E). Two mutant plasmids were constructed to examine the minimal number of lysine residues required for the role of this domain in the function of protein 2B. In mutant 2B-K[41]L, lysine 41 is replaced with a leucine residue. In mutant 2B-K[41,44]L, both lysine 41 and lysine 44 are replaced with leucine residues. In the remaining two substitution mutants, the importance of the negatively charged glutamic acid 40 was examined. In these mutants, glutamic acid 40 was replaced with either a lysine (2B-E[40]K) or an aspartic acid (2B-E[40]D) residue. In the three insertion mutants (2B-ins[41]L, 2B-ins[44]L, and 2B-ins[48]L), hydrophobic leucine residues were introduced at aa 41, 44, and 48, respectively. The insertion of

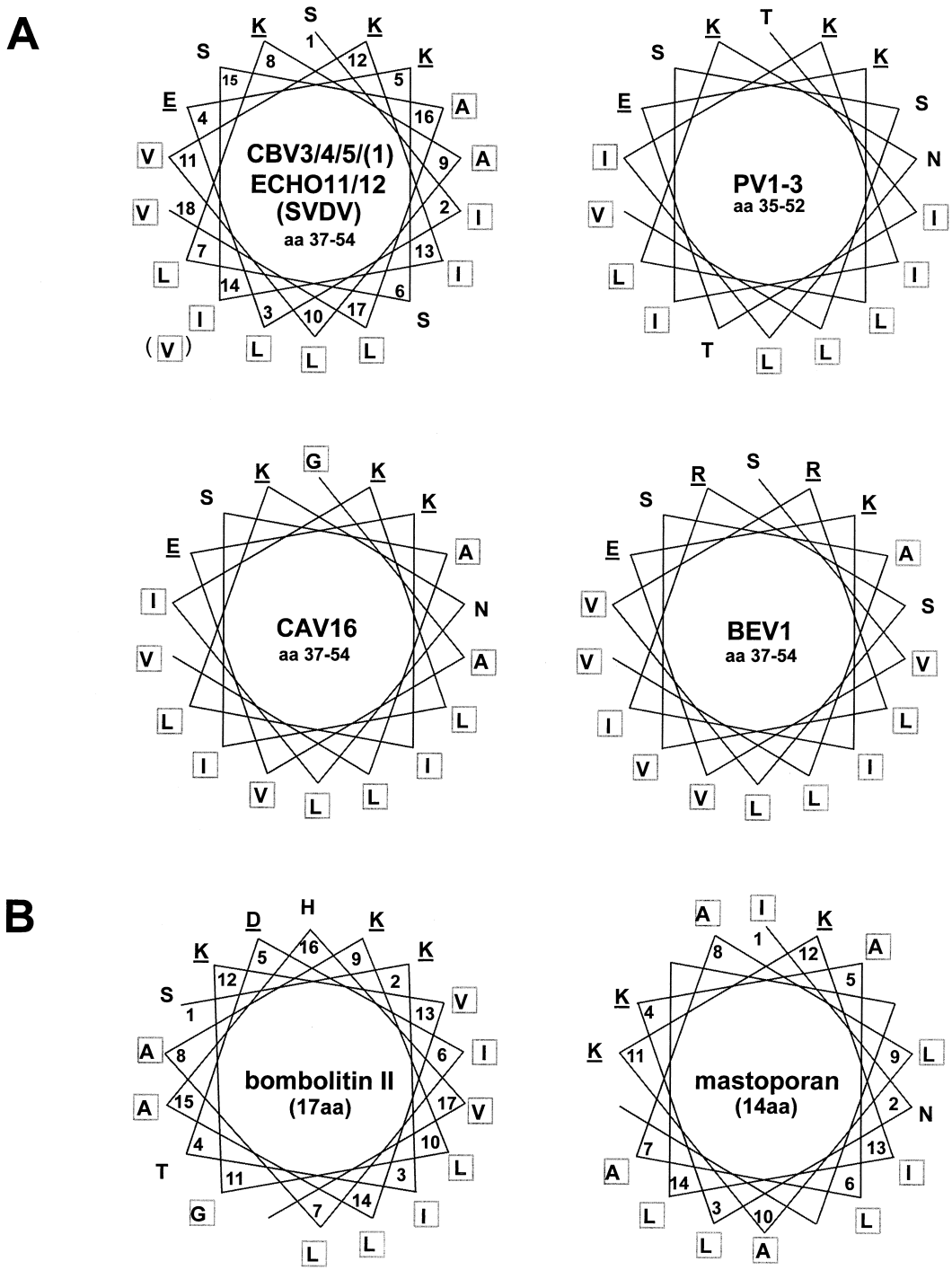

FIG. 2. (A) Helical wheel diagrams of the putative amphipathic helices found in the 2B proteins of several enteroviruses according to the method of Schiffer and Edmundson (40). Positively charged (R and K) and negatively charged (D and E) residues are underlined. Hydrophobic amino acids are boxed. Abbreviations: CBV, coxsackie B virus; CAV, coxsackie A virus; ECHO, echovirus; SVDV, swine vesicular disease virus; PV, poliovirus; BEV, bovine enterovirus. (B) Helical wheel diagrams of lytic polypeptides bombolitin II, a heptadecapeptide isolated from the venom of bumblebee *M. pennsylvanicus* (4), and mastoporan, a tetradecapeptide isolated from the venom of the wasp *Vespula lewisii* (23).

these residues leads to the dispersion of the charged residues and, as a consequence, the disruption of the narrow polar face of the putative amphipathic helix (Fig. 3B), without disturbing the overall hydrophobicity of the domain (Fig. 3A).

Effect of the mutations on virus growth. The effect of the mutations on virus viability was studied by transfection of BGM cells with RNA transcripts. For each mutant, eight transfections were performed. After transfection, the cells were incubated at either 33 or 36°C. In case no virus growth was observed after 5 days, the cells were subjected to three cycles of freezing and thawing and 250 μl was passaged to fresh BGM cell monolayers, which were incubated for another three

A

plasmid	amino acid sequence	aa 37-54 mom.	aa 37-54 hyd.	aa 40-50 mom.	aa 40-50 hyd.	plaque phenotype
	- + + +					
pCB3/T7 wt	S I L E K S L K A L V K I I S A L V	0.54	0.33	0.67	0.11	
	40 45 50					
2B-K[41,44,48]R	. . . . R . . R . . . R	0.69	0.16	0.93	-0.18	wild-type
2B-K[41,44,48]E	. . . . E . . E . . . E	0.43	0.46	0.49	0.31	-
2B-K[41]L	. . . . L	0.43	0.48	0.48	0.34	small
2B-K[41,44]L	. . . . L . . L	0.30	0.62	0.27	0.57	minute
2B-E[40]K	. . . K	0.56	0.29	0.70	0.04	-
2B-E[40]D	. . . D	0.53	0.32	0.68	0.09	wild-type
2B-ins[41]L	. . . .L.	0.30	0.37	0.45	0.08	-
2B-ins[44]L	. . . . . .L.	0.37	0.37	0.56	0.08	-
2B-ins[48]L	. . . . . .L.	0.28	0.37	0.42	0.08	-

B

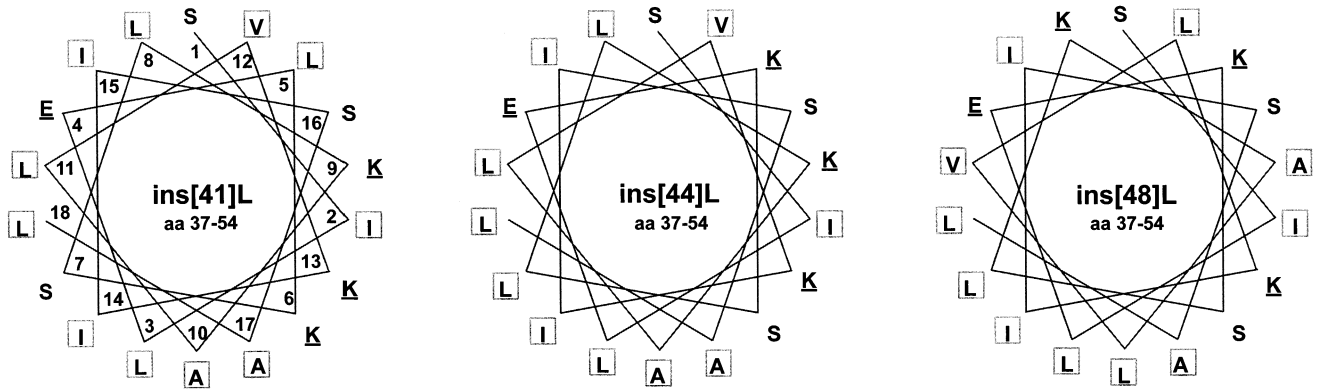

FIG. 3. (A) Partial amino acid sequence (residues 37 to 54) and the hydrophobic moment and hydrophobicity values of the 2B proteins encoded by wild-type pCB3/T7 and the pCB3/T7-derived mutant plasmids. The effects of the mutations on the hydrophobic moment (mom.) and hydrophobicity (hyd.) of both the entire 18-aa amphipathic helix and the most-amphipathic 11-aa segment (aa 40 to 50) are shown. Furthermore, the effects of the mutations on virus growth are summarized. (B) Helical wheel diagrams of the insertion mutants 2B-ins[41]L, 2B-ins[44]L, and 2B-ins[48]L, containing leucine insertions at residue positions 41, 44, and 48, respectively.

(36°C) or five (33°C) days. Viruses were obtained consistently with RNA transcripts carrying mutations K[41,44,48]R, K[41]L, K[41,44]L, and E[40]D. Plaque assays were performed, and four individual plaques were isolated from each mutant virus. Sequence analysis of the 2B coding region of these viruses showed that the mutations introduced by site-directed mutagenesis were retained in the viral RNA and that no other amino acid replacements had occurred. These viruses were designated vCB3-2B-K[41,44,48]R, vCB3-2B-K[41]L, vCB3-2B-K[41,44]L, and vCB3-2B-E[40]D, respectively. No virus growth was observed upon transfection of BGM cells with RNA transcripts containing mutation K[41,44,48]E, ins[41]L, ins[44]L, or ins[48]L. To ensure that the nonviability of these mutations was not due to additional mutations in the plasmid DNA, new constructs carrying these mutations were made and RNA transcripts were assayed for their viability. Consistent with our initial results, no virus growth was observed following transfection.

Upon transfection with RNA transcripts of mutant 2B-E[40]K, virus growth was observed in only two of the eight transfected cultures. In one cell culture, virus growth was observed on the second day posttransfection. Sequence analysis

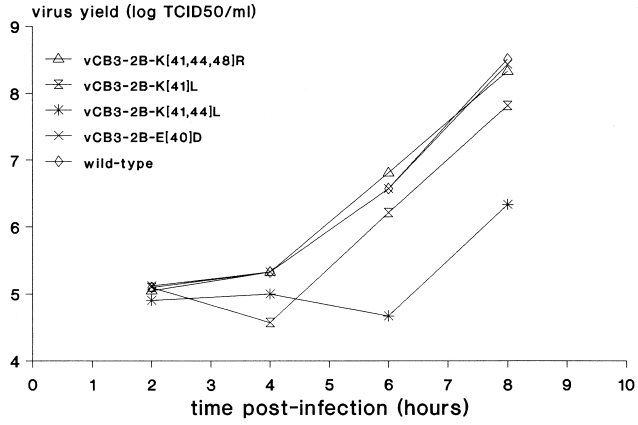

FIG. 4. Single-cycle growth curves of wild-type and mutant viruses vCB3-2B-K[41,44,48]R, vCB3-2B-K[41]L, vCB3-2B-K[41,44]L, and vCB3-2B-E[40]D. BGM cells were infected at a MOI of 1, incubated at 36°C, and harvested at 2, 4, 6, and 8 h postinfection. Viruses were released from the infected cells by three cycles of freezing and thawing, and the virus titers were determined by titration on BGM cells at 36°C. $TCID_{50}$, 50% tissue culture infective dose.

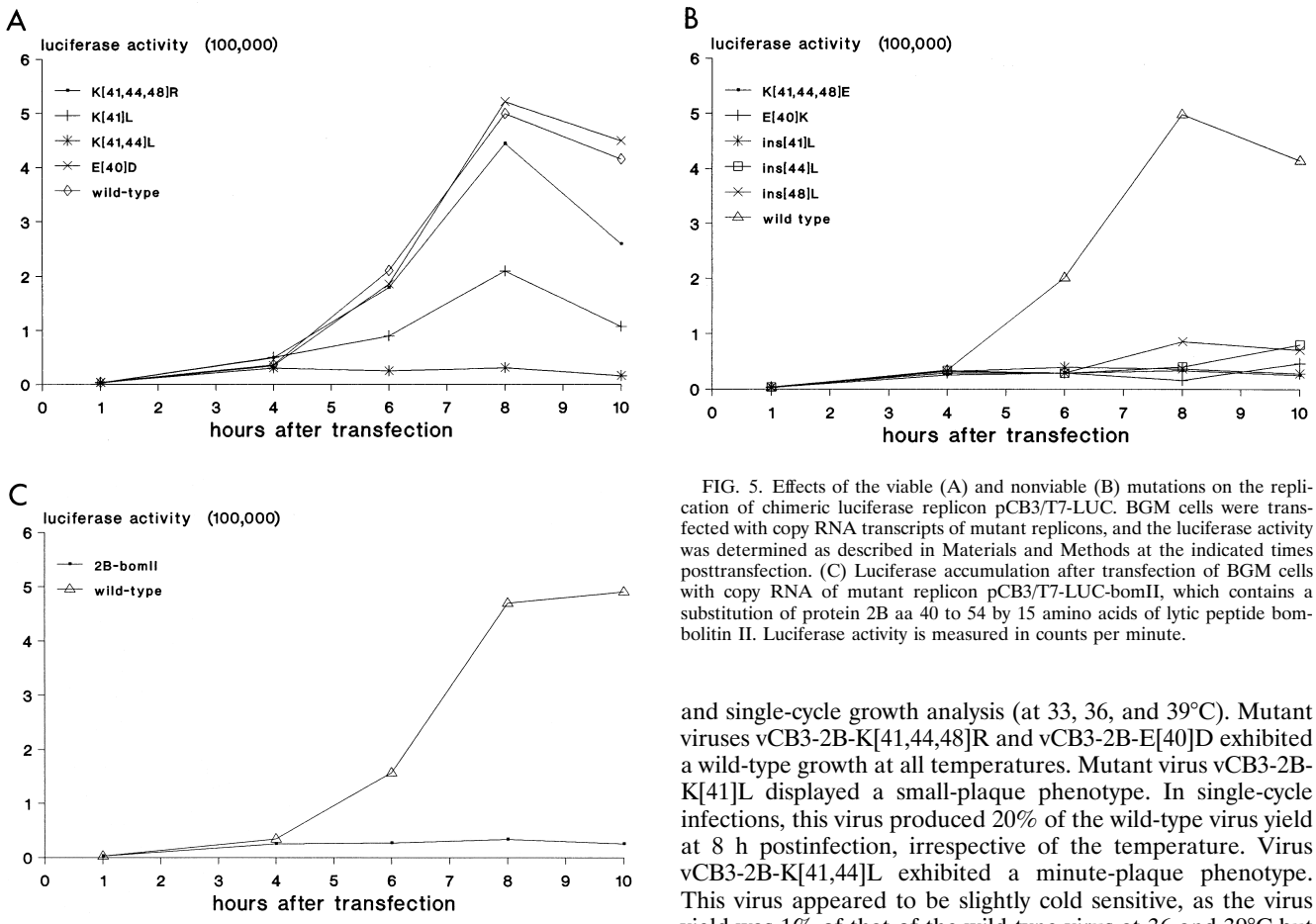

FIG. 5. Effects of the viable (A) and nonviable (B) mutations on the replication of chimeric luciferase replicon pCB3/T7-LUC. BGM cells were transfected with copy RNA transcripts of mutant replicons, and the luciferase activity was determined as described in Materials and Methods at the indicated times posttransfection. (C) Luciferase accumulation after transfection of BGM cells with copy RNA of mutant replicon pCB3/T7-LUC-bomII, which contains a substitution of protein 2B aa 40 to 54 by 15 amino acids of lytic peptide bombolitin II. Luciferase activity is measured in counts per minute.

of the 2B coding region of these viruses showed that the introduced lysine 40 (AAG) reverted to the original glutamic acid (GAG) by a single point mutation. No cytopathic effect was observed in the remaining seven transfected cell cultures. Upon passage of these cultures, however, virus growth became visible in one of the cultures grown at 33°C. Sequence analysis of the 2B coding region of these viruses showed that the introduced lysine 40 (AAG) was retained in the viral RNA and that no other mutations had occurred. This finding was rather unexpected, because the lack of virus growth in the other cultures suggested that a reversion of the introduced mutation to a more favorable residue or a second-site compensating mutation in protein 2B had occurred. To investigate whether mutation E[40]K indeed allows virus growth and to exclude the possibility that the phenotype of the original mutation was influenced by an additional mutation elsewhere in the plasmid DNA, which might have arisen during plasmid construction, virus nt 3837 to 4238 (which were found to be identical to those of plasmid 2B-E[40]K) were amplified, cut with *Spe*I and *Bss*HII, and cloned into wild-type pCB3/T7. BGM cells were transfected with RNA transcripts of several independently reconstructed plasmids. However, no virus growth was observed in any of the transfected cell cultures. These data strongly suggest that mutation E[40]K is nonviable and that the viability and phenotype of the isolated virus are due to a second-site mutation outside 2B. For this reason, the virus was not included in further characterization studies.

Viral growth characteristics were examined by plaque assay and single-cycle growth analysis (at 33, 36, and 39°C). Mutant viruses vCB3-2B-K[41,44,48]R and vCB3-2B-E[40]D exhibited a wild-type growth at all temperatures. Mutant virus vCB3-2B-K[41]L displayed a small-plaque phenotype. In single-cycle infections, this virus produced 20% of the wild-type virus yield at 8 h postinfection, irrespective of the temperature. Virus vCB3-2B-K[41,44]L exhibited a minute-plaque phenotype. This virus appeared to be slightly cold sensitive, as the virus yield was 1% of that of the wild-type virus at 36 and 39°C but only 0.05% of that of the wild-type virus at 33°C. Figure 4 shows the viral growth curves of the mutant viruses at 36°C. The effects of the mutations on virus growth are summarized in Fig. 3.

Effect of the mutations on RNA replication. In a previous study, we reported the construction and use of chimeric subgenomic replicon pCB3/T7-LUC, which carries the luciferase gene in place of the P1 protein coding region, to study RNA replication (46). Upon transfection of BGM cells with RNA transcripts of pCB3/T7-LUC, a triphasic pattern of luciferase accumulation was observed; luciferase activity increased as a result of translation of the input RNA (phase I), remained constant until the fifth hour posttransfection (phase II), and showed a second increase as a result of the translation of newly synthesized chimeric RNA strands (phase III). That luciferase accumulation indeed reflected viral RNA replication was demonstrated by measuring replicon RNA levels by dot blot hybridization (data not shown). To study the effect of the mutations on RNA replication, the *Spe*I-to-*Bss*HIII fragments of the mutant plasmids were cloned in replicon pCB3/T7-LUC. BGM cells were transfected with RNA transcripts of the mutant replicons, and luciferase activity was determined at 1, 4, 6, 8, and 10 h posttransfection. The effects of the viable mutations on RNA replication are shown in Fig. 5A. The introduction of mutation K[41]L resulted in a reduced level of RNA replication, as the increase in luciferase activity was only fourfold, whereas the increase in luciferase accumulation was 10- to 20-fold in the case of mutations K[41,44,48]R and E[40]D and wild-type pCB3/T7-LUC. Mutation K[41,44]L caused a more drastic reduction in RNA synthesis, as demonstrated by the

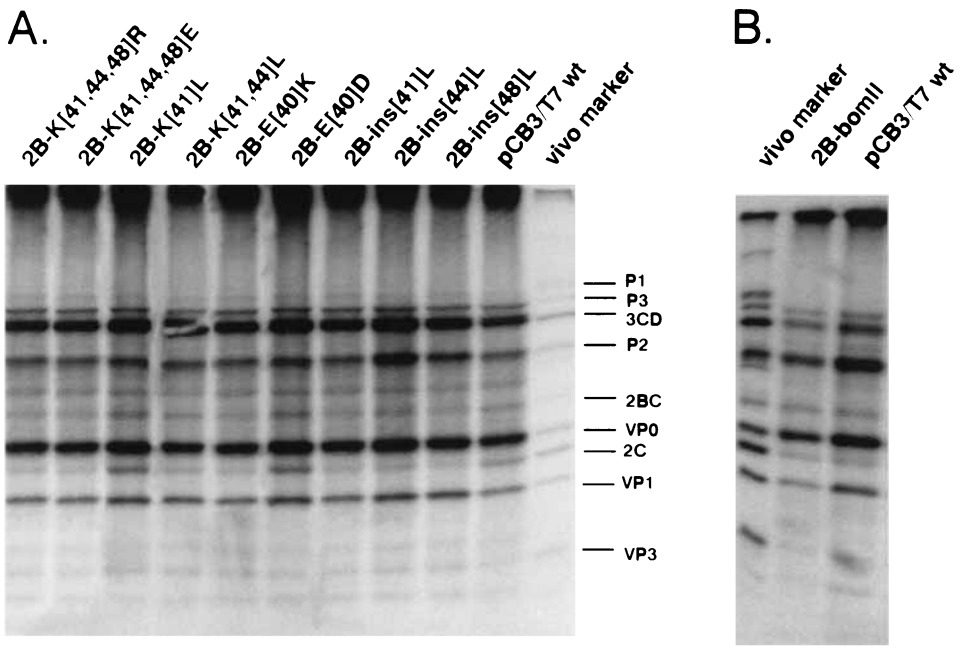

FIG. 6. In vitro translation reactions of RNA transcripts derived from the plasmids carrying mutations in the putative amphipathic helix (A) and plasmid 2B-bomII (B). Circular plasmid DNA (0.5 μg) was incubated for 3 h in TNT rabbit reticulocyte lysate, a coupled transcription-translation system, supplemented with HeLa cell initiation factors. The [^{35}S]methionine-labeled translation products were analyzed on an SDS–12.5% polyacrylamide minigel. An extract from wild-type-virus-infected cells, labeled with [^{35}S]methionine for 30 min at 4 h postinfection, was used as a marker.

absence of a notable increase in luciferase activity. The failure to detect a low level of RNA replication is most likely due to the low infectivity of the RNA transcripts, as has been explained previously (46). The effects of the nonviable mutations on replicon replication are shown in Fig. 5B. This figure shows that each of the mutations, K[41,44,48]E, E[40]K, ins[41]L, ins[44]L, and ins[48]L, disturbed RNA replication but not translation of the chimeric RNA transcripts. The stability of the RNA appeared to be unaffected by the mutations, as the activity of luciferase, which is an unstable enzyme in vivo, remained constant up to 10 h posttransfection, suggesting a balance between translation of the input RNA and luciferase degradation.

Analysis of in vitro protein synthesis and polyprotein processing. In vitro translation reactions were performed to examine whether any of the mutations affected polyprotein synthesis and processing. RNA was synthesized and translated in a single reaction mixture, using T7 TNT rabbit reticulocyte lysate, a combined transcription-translation system, supplemented with HeLa cell initiation factors. The patterns of ^{35}S-

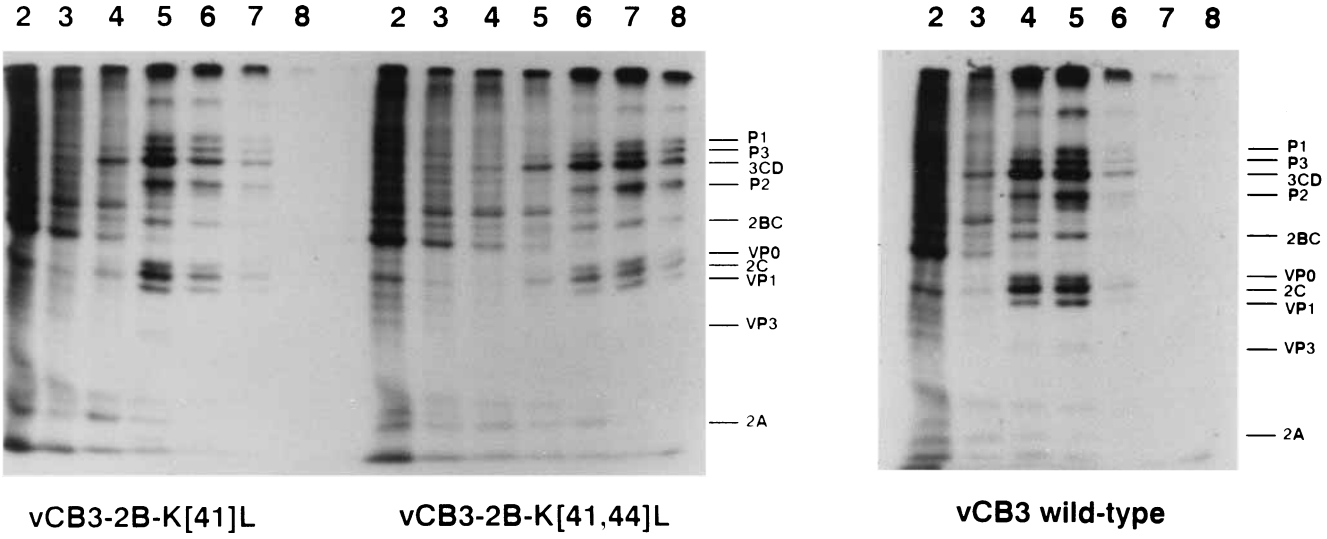

FIG. 7. Protein synthesis in BGM cells infected with vCB3-2B-K[41]L, vCB3-2B-K[41,44]L, and wild-type virus. Cells were infected at a MOI of 25, grown at 36°C, and incubated with methionine- and serum-free MEM containing 10 μCi of Tran^{35}S-label (a mixture of [^{35}S]methionine and [^{35}S]cysteine) at various times postinfection (indicated [in hours] above each lane). After a 30-min labeling period, the cells were washed and lysed. The labeled proteins were analyzed on an SDS–12.5% polyacrylamide minigel.

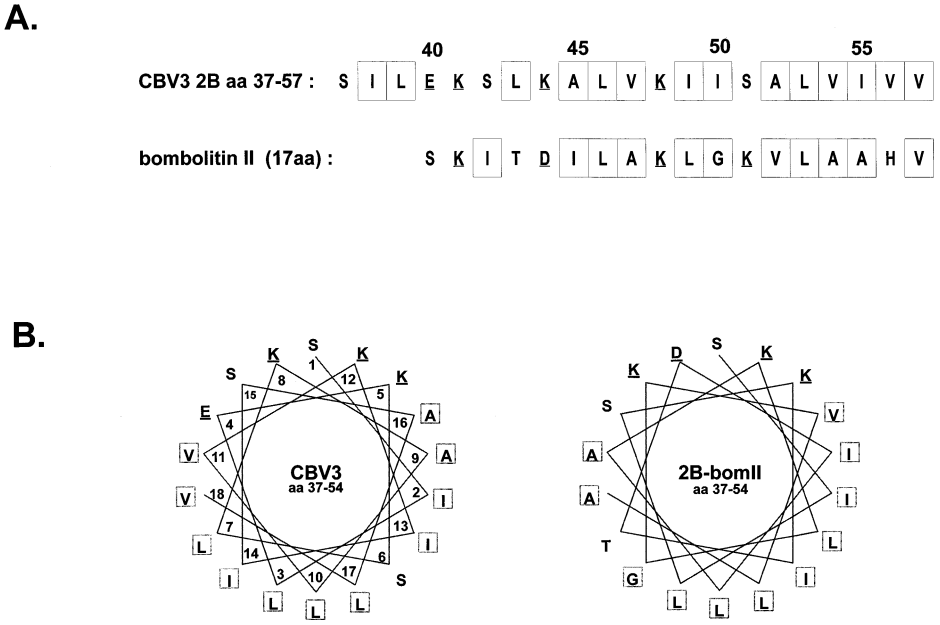

FIG. 8. (A) Alignment of aa 37 to 57 of CBV3 protein 2B with the amino acid sequence of cationic α-helical lytic polypeptide bombolitin II (4). Positively charged (R and K) and negatively charged (D and E) residues are underlined. Hydrophobic amino acids are boxed. (B) Helical wheel diagrams showing the amphipathic α-helices (aa 37 to 54) of wild-type CBV3 protein 2B (as encoded in plasmid pCB3/T7) and chimeric protein 2B encoded in plasmid 2B-bomII. In plasmid 2B-bomII, nt 3862 to 3906 (coding for aa 40 to 54) are replaced with 45 nt encoding the first 15 aa of bombolitin II.

labeled proteins translated from the mutant pCB3/T7 RNAs are shown in Fig. 6A. The results demonstrate that none of the mutations caused abnormalities in polyprotein processing. All cleavage products migrated with a correct mobility, and the translation patterns of all mutants were similar to that of wild-type pCB3/T7. Although it cannot be excluded that minor differences in the levels of the replication proteins contribute to the viral phenotypes, these results suggest that it is unlikely that the defects in vRNA synthesis caused by the nonviable mutations K[41,44,48]E, E[40]K, ins[41]L, ins [44]L, and ins[48]L and the reductions in vRNA synthesis caused by the viable mutations K[41]L and K[41,44]L are due to defects in polyprotein processing.

Time course of protein synthesis in infected cells. The possibility that the reductions in virus yield and vRNA synthesis caused by mutations K[41]L and K[41,44]L are due to a reduced level of viral protein synthesis was considered. To examine this possibility, we studied viral protein synthesis in vivo. BGM cells were infected with either mutant or wild-type virus at a MOI of 25 and labeled with [^{35}S]methionine for 30 min at various times postinfection. Figure 7 shows the electrophoretic analysis of the labeled proteins. From this figure, it can be seen that all viruses cause a similar shutoff of host protein synthesis but that viral protein synthesis is delayed in cells infected with the mutant viruses. Viral protein synthesis in wild-type-virus-infected cells peaks at 4 to 5 h postinfection and is inhibited from the sixth hour. In cells infected with the small-plaque virus vCB3-2B-K[41]L, viral protein synthesis peaks at 5 to 6 h postinfection, whereas in cells infected with the minute-plaque mutant vCB3-2B-K[41,44]L, viral protein synthesis is even delayed up to 6 to 7 h postinfection. These differences probably reflect a delayed growth of the mutant viruses and, as a result, a delay in cytopathic effect. Although viral protein synthesis is delayed in the mutant-infected cells, the level of viral protein synthesis is similar to that in wild-type-virus-infected cells, suggesting that it is unlikely that the reductions in growth and vRNA synthesis of these viruses are due to an impaired level of viral protein production.

Replacement of the amphipathic helix with lytic peptide bombolitin II. After having demonstrated that a cationic amphipathic α-helix is required for a function of protein 2B, we tested whether the α-helix could be functionally replaced by the cationic lytic polypeptide bombolitin II. Bombolitin II is a heptadecapeptide (Ser-Lys-Ile-Thr-Asp-Ile-Leu-Ala-Lys-Leu-Gly-Lys-Val-Leu-Ala-His-Val) identified in the venom of the bumblebee *Megabombus pennsylvanicus* (4). A helical wheel representation of this peptide shows that it can form an amphipathic α-helix with a narrow polar face of six amino acids containing three lysine residues, one negatively charged aspartic acid, and two polar residues (Fig. 2B). Alignment of the amino acid sequences of both helices showed that bombolitin II resembles aa 40 to 56 of CBV3 protein 2B (Fig. 8A). We have replaced the nucleotide sequence encoding aa 40 to 54 with a sequence encoding the first 15 aa of bombolitin II. The nucleotide sequence of the introduced PCR product was verified, and the resulting plasmid was designated 2B-bomII. A helical wheel diagram of aa 37 to 54 of this chimeric plasmid is shown in Fig. 8B. In vitro translation of RNA from this plasmid showed a processing pattern that was similar to that produced by wild-type pCB3/T7 RNA (Fig. 6B). To study the viability of this chimeric construct, BGM cells were transfected with T7 RNA polymerase-generated RNA transcripts. A total of 10 transfections, including passage of the transfected cell cultures to fresh cells, was performed. In none of the transfected cell cultures, however, was virus growth observed. The *Spe*I-to-*Bss*HII fragment of 2B-bomII was introduced in subgenomic replicon pCB3/T7-LUC to study RNA replication. Analysis of luciferase accumulation following the transfection of BGM cells with copy RNA transcripts demonstrated a defect in replication of the replicon RNA (Fig. 5C). This finding suggests that despite the structural similarities between the amphipathic helix motifs, the cationic α-helix of bombolitin II cannot fulfill

the function of the cationic amphipathic α-helix of CBV3 protein 2B in vRNA synthesis.

DISCUSSION

Membrane permeabilization is a phenomenon that occurs during the late phase of the replication cycle of most cytolytic viruses. This modification of the membrane is dependent on viral gene expression. A number of viral proteins involved in modifying membrane permeability have been identified in recent years, and a general term for this kind of proteins has been introduced: viroporins (13). A general feature of these viroporins is the presence of amphipathic helix motifs, which are thought to destabilize the membrane integrity by interacting with the lipid bilayer. Until recently, the identity of an enterovirus viroporin was unknown. Upon expression of the poliovirus nonstructural proteins in *Escherichia coli*, it was found that both proteins 2B and 3A modified the bacterial cell membrane (31). Very recently, it has been shown that poliovirus protein 2B, but not protein 3A, permeabilizes the plasma membrane in eucaryotic cells (16), suggesting that protein 2B is most probably the enterovirus viroporin. Consistent with this idea, we have identified an amphipathic helix motif in protein 2B that is conserved among all enteroviruses (Fig. 2A). The arrangement of charged residues in a narrow hydrophilic face and the predominant occurrence of cationic lysine residues are typical of amphipathic helices formed by members of the class of lytic polypeptides.

In this study, we have examined the functional and structural roles of the putative amphipathic helix in CBV3 protein 2B. Nine mutant cDNAs were constructed by site-directed mutagenesis. The results obtained with the mutants carrying substitutions of the lysine residues (aa 41, 44, and 48) suggest that cationic residues are required for the role of the amphipathic helix in the function of protein 2B. Replacement of the lysine residues with arginine residues (K[41,44,48]R) did not affect virus growth, whereas substitution of the lysine residues with negatively charged glutamic acid residues (K[41,44,48]E) was nonviable because of defects in vRNA replication. Substitution of lysine 41 by a leucine residue (K[41]L) yielded a small-plaque virus that produced 20% of the wild-type virus yield in a single-cycle infection, because of a reduction in vRNA synthesis. Substitution of both lysine 41 and lysine 44 by leucine residues (K[41,44]L) yielded a minute-plaque virus that produced only 1% of the wild-type virus yield in a single-cycle infection, because of a more severe defect in vRNA synthesis. These results suggest that the presence of cationic residues is a major determinant of the function of the amphipathic helix in protein 2B. The introduction of negatively charged residues in the hydrophilic face of the helix disrupts the function of protein 2B, although the amphipathic helix containing mutation K[41,44,48]E displays a hydrophobic moment that is equal to or even larger than the moments of the helices containing mutation K[41]L or K[41,44]L, respectively (Fig. 3A).

Two substitution mutations were introduced to investigate the importance of the negatively charged glutamic acid 40 in the function of the amphipathic helix. The introduction of a lysine residue (E[40]K) was highly detrimental for virus growth, although this mutation has virtually no effect on the amphipathy of the α-helix (Fig. 3A). Viruses containing this mutation were isolated on only one occasion. The failure to recover viruses from simultaneously transfected cell cultures suggested that a second-site compensating mutation might have occurred. No such mutation was found in protein 2B. Reconstruction of the mutation into wild-type cDNA followed by transfection of cells with RNA transcripts of the resulting clones did not give rise to virus growth. These data are indicative of the occurrence of an additional second-site mutation outside 2B. Experiments to test this possibility are currently in progress. The wild-type growth characteristics of viruses carrying a replacement of glutamic acid 40 with a negatively charged aspartic acid (E[40]D) demonstrate that a negatively charged residue is preferred at this position. The reason for the preference for a negatively charged residue in the hydrophilic face of this cationic amphipathic α-helix is unknown. None of the substitution mutations interfered with viral protein synthesis and polyprotein processing, indicating that the effects of these mutations on virus growth are primarily attributable to defects in vRNA replication.

The importance of the amphipathic character of the helix for the function of protein 2B was demonstrated by characterization of the three insertion mutants. Leucine residues were inserted between the charged residues (ins[41]L, ins[44]L, and ins[48]L), such that the amphipathy of the α-helix was severely disturbed whereas its mean hydrophobicity was unaffected. These mutations caused severe defects in vRNA synthesis and were all nonviable. The hydrophobic moments of these helices were similar to that containing mutation K[41,44]L (Fig. 3A). A main difference, however, is that because of the insertion mutations, the charged residues are dispersed and even located in the hydrophobic part of the helix, which probably interferes with the hydrophobic interaction with the membrane, whereas the narrow hydrophilic face and the hydrophobic part of the α-helix are maintained by mutation K[41,44]L. None of the insertion mutations affected the synthesis and processing of the viral protein, indicating that they primarily affected vRNA synthesis. Altogether, the results obtained with both the substitution and insertion mutants suggest that an amphipathic α-helix containing predominantly cationic lysine residues in a narrow hydrophilic face is a major structural determinant involved in a function of protein 2B, and possibly its precursor 2BC, in vRNA replication.

The structure of the cationic amphipathic α-helices found in enterovirus protein 2B shows close similarities to that of the cationic amphipathic α-helical peptides that form the class of lytic polypeptides (41). Most of these short cationic lytic polypeptides have been identified in the venom of insects or the skin of amphibia and are involved in an antibacterial defense system. Two models of action have emerged from the structural and functional studies on these peptides (reviewed in reference 6). In one model, the cytolytic helices form aqueous channels by spanning the membrane and forming oligomers, exposing their hydrophobic sides to the lipid bilayer and their hydrophilic faces to the aqueous pores. Although anion selectivity may be predicted, membrane currency measurements have demonstrated that cationic peptides can form either anion-selective (15, 17, 45) or cation-selective ion channels (1, 24, 44). These channels produce ionic imbalances which will ultimately result in colloid osmotic lysis. A second model proposes that these peptides produce lysis by disrupting the phospholipid structure of the membrane by lying parallel to the membrane and perturbing the membrane, making the membrane phospholipids more susceptible to enzymatic degradation by phospholipases (6, 41). The resulting lesions in the membrane would allow a flux of ions, causing the ionic imbalances that are responsible for lysis of the cell.

The modification of the plasma membrane that occurs during an enterovirus infection is such that both gradients of sodium and potassium are disturbed and small nonpermeative translation inhibitors like hygromycin B and edeine can enter the virus-infected cells (13). Later in infection, the cellular membrane becomes more severely disrupted, and enzymes and

sugars can also leak out of the infected cells (13). The initial permeability of the plasma membrane for both monovalent cations and small translation inhibitors suggests that pores or membrane lesions, rather than a specific ion pump, are formed. By analogy with the lytic polypeptides, protein 2B may form transmembrane cation-selective pores or lie collateral to the membrane, making the phospholipids more accessible to the action of phospholipases. Both mechanisms would account for the observed ion fluxes across the membrane, causing the ionic imbalances that may be responsible for a further destabilization of the membrane. Many cytolytic viruses have been reported to increase phospholipase activity. In poliovirus-infected cells, choline and phosphorylcholine are released in the culture medium and the levels of diacylglycerol and inositol triphosphate in the cytoplasm are increased from the third hour postinfection (21). Although this finding suggests that the membrane modification may be caused by phospholipases, the possibilities that protein 2B still forms transmembrane pores and that the integration of these pores is responsible for disturbing the integrity of the membrane and the activation of the phospholipases cannot be excluded.

Although protein 2B has a profound effect on the permeability of the plasma membrane, it should be emphasized that there is no experimental proof for an interaction of protein 2B with the plasma membrane. Electron microscopic studies using immunocytochemistry have shown that proteins 2B, 2C, and 2BC of poliovirus are contained exclusively at the endoplasmic reticulum membrane or the surface of the endoplasmic reticulum-derived membrane vesicles that surround the viral replication complexes (8). Intracellular localization of individual expressed poliovirus protein 2B in eucaryotic cells showed a disseminated distribution throughout the cytoplasm (2). These findings suggest that protein 2B interacts with intracellular membranes rather than with the plasma membrane. On the basis of these observations, an alternative mechanism for the induction of the plasma membrane modification may be proposed. Because of its ionophoric or membrane-perturbing properties, protein 2B may permeabilize endoplasmic reticulum membranes and cause the leakage of stored calcium ions into the cytosol. The consequences of a permanent increase in cytosolic calcium concentration for cellular metabolism and virus reproduction are unknown. However, as calcium is a regulator of a broad spectrum of physiological processes, it is likely that an increased calcium level is highly toxic for an array of cellular structures and processes. Increased cytosolic calcium levels in rotavirus (32), Semliki Forest virus (37), cytomegalovirus (34), and recently also in poliovirus-infected cells (25) have been demonstrated. The possible role of the alterations in calcium ion concentrations in viral replication, membrane permeabilization, and cell lysis, however, remains to be elucidated.

Mutations that disrupt the cationic amphipathic α-helix in protein 2B cause primary defects in vRNA synthesis, suggesting that the initial consequence of the membrane modification (i.e., the efflux of potassium ions and the influx of sodium ions or, alternatively, the efflux of calcium) is a prerequisite for vRNA replication. However, the possibility that the cationic amphipathic helix is also required for the second function that has been attributed to protein 2B, i.e., the inhibition of cellular protein secretion, cannot be excluded. It has been proposed that this inhibition is involved in the accumulation of membrane vesicles on which positive-strand RNA synthesis occurs (16). Permeabilization of membranes may be required for this function, by causing either an altered ionic environment that may be inhibitory to protein transport or a nonspecific leakiness of intracellular organelle membranes and the loss of molecules crucial for transport. A disruption of the cationic amphipathic helix may interfere with the accumulation of the virus-induced membrane vesicles that are required for the formation of the viral replication complexes and thereby may be responsible for the defects in vRNA replication.

Although the results presented in this paper indicate that the cationic amphipathic α-helix in protein 2B is an important requirement for its function in vRNA synthesis, replacement of this structural motif with the cationic amphipathic helix of lytic peptide bombolitin II resulted in a nonfunctional protein 2B. Both amphipathic helices contain a small hydrophilic face formed by three lysines, one negatively charged residue, and two polar residues (Fig. 2). The nonviability of this chimeric construct (2B-bomII) suggests that the position of the charged residues in the helix may be crucial either for the formation of a cation-specific pore or for the membrane-perturbing capacity. Alternatively, alterations in the amino acid sequence of this domain may interfere with a possible interaction of the putative amphipathic helix with another membrane-interacting domain of CBV3 protein 2B. Potential candidates for such an interaction are the N-terminal 16 aa, which also have considerable potential to form an amphipathic α-helix (Fig. 1), and the hydrophobic domain, formed by aa 63 to 80, which contains an amino acid composition and hydrophobicity features that are characteristic of multimeric transmembrane regions (46). Either of these domains may, together with the cationic amphipathic α-helix, cooperatively be involved in the formation of a cation-specific pore. Additional mutational analysis and analysis of the effects of individually expressed mutant 2B proteins on membrane permeability and protein secretion are required for a better understanding of the involvement of protein 2B in membrane modification and virus replication.

REFERENCES

1. **Agawa, Y., S. Lee, S. Ono, H. Aoyagi, M. Ohno, T. Taniguchi, K. Anzai, and Y. Kirino.** 1991. Interaction with phospholipid bilayers, ion channel formation, and antimicrobial activity of basic amphipathic α-helical model peptides of various chain lengths. J. Biol. Chem. **266:**20218–20222.
2. **Aldabe, R., and L. Carrasco.** 1995. Induction of membrane proliferation by poliovirus proteins 2C and 2BC. Biochem. Biophys. Res. Commun. **206:**64–76.
3. **Andino, R., G. E. Rieckhof, P. L. Achacoso, and D. Baltimore.** 1993. Poliovirus RNA synthesis utilizes an RNP complex formed around the 5′ end of viral RNA. EMBO J. **12:**3587–3598.
4. **Argiolas, A., and J. J. Pisano.** 1985. Bombolitins, a new class of mast cell degranulating peptides from the venom of bumblebee *Megabombus pennsylvanicus*. J. Biol. Chem. **260:**1437–1444.
5. **Baltimore, D.** 1968. Structure of the poliovirus replicative intermediate RNA. J. Mol. Biol. **32:**359–368.
6. **Bernheimer, A. W., and B. Rudy.** 1986. Interactions between membranes and cytolytic peptides. Biochim. Biophys. Acta **864:**123–141.
7. **Bienz, K., D. Egger, and L. Pasamontes.** 1987. Association of polioviral proteins of the P2 genomic region with the viral replication complex and virus-induced membrane synthesis as visualized by electron microscopic immunocytochemistry and autoradiography. Virology **160:**220–226.
8. **Bienz, K., D. Egger, and T. Pfister.** 1994. Characteristics of the poliovirus replication complex. Arch. Virol. **9**(Suppl.)**:**147–157.
9. **Bienz, K., D. Egger, Y. Rasser, and W. Bossart.** 1983. Intracellular distribution of poliovirus proteins and the induction of virus-specific cytoplasmic structures. Virology **131:**39–48.
10. **Bienz, K., D. Egger, M. Troxler, and L. Pasamontes.** 1990. Structural organization of poliovirus RNA replication is mediated by viral proteins of the P2 genomic region. J. Virol. **64:**1156–1163.
11. **Bonneau, A.-M., and N. Sonenberg.** 1987. Proteolysis of the p220 component of the cap-binding protein complex is not sufficient for complete inhibition of host cell protein synthesis after poliovirus infection. J. Virol. **61:**986–991.
12. **Carrasco, L.** 1978. Membrane leakiness after viral infection and a new approach to the development of antiviral agents. Nature (London) **272:**694–699.
13. **Carrasco, L., L. Pérez, A. Irurzun, J. Lama, F. Martínez-Abarca, P. Rodríguez, R. Guinea, J. L. Castrillo, M. A. Sanz, and M. J. Ayala.** 1993. Modification of membrane permeability by animal viruses, p. 283–305. *In* L. Carrasco, N. Sonenberg, and E. Wimmer (ed.), Regulation of gene expres-

sion in animal viruses. Plenum Press, New York.
14. **Cho, M. W., N. Teterina, D. Egger, K. Bienz, and E. Ehrenfeld.** 1994. Membrane rearrangement and vesicle induction by recombinant poliovirus 2C and 2BC in human cells. Virology **202:**129–145.
15. **Christensen, B., J. Fink, R. B. Merriefield, and D. Mauzerall.** 1988. Channel-forming properties of cecropins and related model compounds incorporated into planar lipid membranes. Proc. Natl. Acad. Sci. USA **85:**5072–5076.
16. **Doedens, J. R., and K. Kirkegaard.** 1995. Inhibition of cellular protein secretion by poliovirus proteins 2B and 3A. EMBO J. **14:**894–907.
17. **Duclohier, H., G. Molle, and G. Spach.** 1989. Antimicrobial peptide magainin I from Xenopus skin forms anion-permeable channels in planar lipid bilayers. Biophys. J. **56:**1017–1021.
18. **Ehrenfeld, E.** 1982. Poliovirus-induced inhibition of host-cell protein synthesis. Cell **28:**435–436.
19. **Eisenberg, D., E. Schwarz, M. Komaromy, and R. Wall.** 1984. Analysis of membrane and surface protein sequences with the hydrophobic moment plot. J. Mol. Biol. **179:**125–142.
20. **Etchison, D., S. C. Milburn, I. Edery, N. Sonenberg, and J. W. B. Hershey.** 1982. Inhibition of HeLa cell protein synthesis following poliovirus infection correlates with the proteolysis of a 222,000 Da polypeptide associated with eukaryotic initiation factor 3 and a cap binding protein complex. J. Biol. Chem. **258:**7236–7239.
21. **Guinea, R., A. Lopez Rivas, and L. Carrasco.** 1989. Modification of phospholipase C and phospholipase A2 activities during poliovirus infection. J. Biol. Chem. **264:**21923–21927.
22. **Harris, K. S., W. Xiang, L. Alexander, W. S. Lane, A. V. Paul, and E. Wimmer.** 1994. Interaction of poliovirus polypeptide $3CD^{pro}$ with the 5′ and 3′ termini of the poliovirus genome. J. Biol. Chem. **269:**27004–27014.
23. **Hirai, Y., T. Yasuhara, H. Yoshida, T. Nakajima, M. Fujino, and C. Kitada.** 1979. A new mast cell degranulating peptide "mastoporan" in the venom of Vespula lewisii. Chem. Pharm. Bull. **27:**1942–1944.
24. **Ide, T., T. Taguchi, T. Morita, M. Sato, K. Ikenaka, S. Aimoto, T. Kondo, H. Hojo, M. Kasai, and K. Mikoshiba.** 1989. Mast cell degranulating peptide forms voltage gated and cation-selective channels in lipid bilayers. Biochem. Biophys. Res. Commun. **163:**155–160.
25. **Irurzun, A., J. Arroyo, A. Alvarez, and L. Carrasco.** 1995. Enhanced intracellular calcium concentration during poliovirus infection. J. Virol. **69:**5142–5146.
26. **Jang, S. K., M. V. Davies, R. J. Kaufman, and E. Wimmer.** 1989. Initiation of protein synthesis by internal entry of ribosomes into the 5′ nontranslated region of encephalomyocarditis virus RNA in vivo. J. Virol. **63:**1651–1660.
27. **Johnson, K. L., and P. Sarnow.** 1991. Three poliovirus 2B mutants exhibit noncomplementable defects in viral RNA amplification and display dosage-dependent dominance over wild-type poliovirus. J. Virol. **65:**4341–4349.
28. **Klump, W. M., I. Bergman, B. C. Müller, D. Ameis, and R. Kandolf.** 1990. Complete nucleotide sequence of infectious coxsackievirus B3 cDNA: two initial 5′ uridine residues are regained during plus-strand RNA synthesis. J. Virol. **64:**1573–1583.
29. **Kräusslich, H. G., M. J. H. Nicklin, H. Toyoda, D. Etchison, and E. Wimmer.** 1987. Poliovirus proteinase 2A induces cleavage of eucaryotic initiation factor 4F polypeptide p220. J. Virol. **61:**2711–2718.
30. **Laemmli, U. K.** 1970. Cleavage of structural proteins during the assembly of the head of bacteriophage T4. Nature (London) **227:**680–685.
31. **Lama, J., and L. Carrasco.** 1992. Expression of poliovirus nonstructural proteins in *Escherichia coli* cells. J. Biol. Chem. **267:**15932–15937.
32. **Michelangeli, F., M. C. Rulz, J. R. del Castillo, J. E. Ludert, and F. Liprandi.** 1991. Effect of rotavirus infection on intracellular calcium homeostasis in cultured cells. Virology **181:**520–527.
33. **Mirzayan, C., and E. Wimmer.** 1994. Biochemical studies on poliovirus polypeptide 2C: evidence for ATPase activity. Virology **199:**176–187.
34. **Nokta, M., D. Eaton, O. S. Steinsland, and T. Albrecht.** 1987. Ca^{2+} responses in cytomegalovirus-infected fibroblasts of human origin. Virology **157:**259–267.
35. **Pelletier, J., and N. Sonenberg.** 1988. Internal initiation of translation of eukaryotic mRNA directed by a sequence derived from poliovirus RNA. Nature (London) **334:**320–325.
36. **Pérez, L., and L. Carrasco.** 1992. Lack of direct correlation between p220 cleavage and the shut-off of host translation after poliovirus infection. Virology **189:**178–186.
37. **Peterhans, E., E. Haenggeli, P. Wild, and R. Wyler.** 1979. Mitochondrial calcium uptake during infection of chicken embryo cells with Semliki Forest virus. J. Virol. **29:**143–152.
38. **Reed, L. J., and H. Muench.** 1938. A simple method of estimating fifty per cent endpoints. Am. J. Hyg. **27:**493–497.
39. **Rodriguez, P. L., and L. Carrasco.** 1993. Poliovirus protein 2C has ATPase and GTPase activities. J. Biol. Chem. **268:**8105–8110.
40. **Schiffer, M., and A. B. Edmundson.** 1967. Use of helical wheels to represent the structures of proteins and to identify segments with helical potential. Biophys. J. **7:**121–135.
41. **Segrest, J. P., H. de Loof, J. G. Dohlman, C. G. Brouillette, and G. M. Anantharamaiah.** 1990. Amphipathic helix motif: classes and properties. Proteins Struct. Funct. Genet. **8:**103–117.
42. **Takeda, N., R. J. Kuhn, C. F. Yang, T. Takegami, and E. Wimmer.** 1986. Initiation of poliovirus plus-strand RNA synthesis in a membrane complex of infected HeLa cells. J. Virol. **60:**43–53.
43. **Takegami, T., B. L. Semler, C. W. Anderson, and E. Wimmer.** 1983. Membrane fractions active in poliovirus RNA replication contain VPg precursor polypeptides. Virology **128:**33–47.
44. **Tosteston, M. T., D. S. Auld, and D. C. Tosteston.** 1989. Voltage-gated channels formed in lipid bilayers by a positively charged segment of the Na-channel polypeptide. Proc. Natl. Acad. Sci. USA **86:**707–710.
45. **Tosteston, M. T., and D. C. Tosteston.** 1981. The sting. Mellitin forms channels in lipid bilayers. Biophys. J. **36:**109–116.
46. **van Kuppeveld, F. J. M., J. M. D. Galama, J. Zoll, and W. J. G. Melchers.** 1995. Genetic analysis of a hydrophobic domain of coxsackie B3 virus protein 2B: a moderate degree of hydrophobicity is required for a *cis*-acting function in viral RNA synthesis. J. Virol. **69:**7782–7790.
47. **Wimmer, E., C. U. T. Helen, and X. Cao.** 1993. Genetics of poliovirus. Annu. Rev. Genet. **27:**353–436.